Retina

# Probing Deposit-Driven Age-Related Macular Degeneration Via Thicknesses of Outer Retinal Bands and Choroid: ALSTAR2 Baseline

Mehdi Emamverdi,[1,3] Charles Vatanatham,[1] Sohaib Fasih-Ahmad,[1] Ziyuan Wang,[1] Zubin Mishra,[1] Anjal Jain,[1] Anushika Ganegoda,[1] Mark E. Clark,[2] Abbas Habibi,[1,3] Maryam Ashrafkhorasani,[1,3] Cynthia Owsley,[2] Christine A. Curcio,[2] Zhihong J. Hu,[1] and SriniVas R. Sadda[1,3]

[1]Doheny Eye Institute, Pasadena, California, United States
[2]Department of Ophthalmology and Visual Sciences, Heersink School of Medicine, University of Alabama at Birmingham, Birmingham, Alabama, United States
[3]Doheny Eye Institute, Department of Ophthalmology, David Geffen School of Medicine, University of California, Los Angeles, California, United States

Correspondence: SriniVas R. Sadda, Doheny Eye Institute, 150 North Orange Grove Blvd, Pasadena, CA 91103, USA;
ssadda@doheny.org.

ME and CV have made equal contributions to this manuscript.

**PURPOSE.** We aimed to identify structural differences in normal eyes, early age-related macular degeneration (AMD), and intermediate AMD eyes using optical coherence tomography (OCT) in a well-characterized, large cross-sectional cohort.

**METHODS.** Subjects $\geq$ 60 years with healthy normal eyes, as well as early or intermediate AMD were enrolled in the Alabama Study on Age-related Macular Degeneration 2 (ALSTAR2; NCT04112667). Using Spectralis HRA + OCT2, we obtained macular volumes for each participant. An auto-segmentation software was used to segment six layers and sublayers: photoreceptor inner and outer segments, subretinal drusenoid deposits (SDDs), retinal pigment epithelium + basal lamina (RPE + BL), drusen, and choroid. After manually refining the segmentations of all B-scans, mean thicknesses in whole, central, inner and outer rings of the ETDRS grid were calculated and compared among groups.

**RESULTS.** This study involved 502 patients, 252 were healthy, 147 had early AMD, and 103 had intermediate AMD eyes (per Age-Related Eye Disease Study [AREDS] 9-step). Intermediate AMD eyes exhibited thicker SDD and drusen, thinner photoreceptor inner segments, and RPE compared to healthy and early AMD eyes. They also had thicker photoreceptor outer segments than early AMD eyes. Early AMD eyes had thinner photoreceptor outer segments than normal eyes but a thicker choroid than intermediate AMD eyes. Using the Beckman scale, 42% of the eyes initially classified as early AMD shifted to intermediate AMD, making thickness differences for photoreceptor outer segments and choroid insignificant.

**CONCLUSIONS.** With AMD stages, the most consistent structural differences involve appearance of drusen and SDD, followed by RPE + BL thickness, and then thickness of photoreceptor inner and outer segments. Structural changes in the transition from aging to intermediate AMD include alterations in the outer retinal bands, including the appearance of deposits on either side of the RPE.

Keywords: optical coherence tomography (OCT), age-related macular degeneration (AMD), aging, drusen, subretinal drusenoid deposit

Age-related macular degeneration (AMD) causes irreversible vision loss among older individuals.[1] Globally, AMD will affect nearly 300 million people by 2040, as the population ages and access to eye care increases.[2,3] AMD affects multiple retinal layers and supporting tissues, including photoreceptors, retinal pigment epithelium (RPE), and Bruch's membrane (BrM) complex, and choroid,[4–7] and pathogenesis is multifactorial. AMD includes an atherosclerosis-like, pro-inflammatory progression at the level of sub-macular BrM, where lipoproteins of RPE origin accumulate throughout adulthood to form high-risk drusen.[8,9] To enable early treatments and preventions, the Alabama Study on Early Age-related Macular Degeneration 2 (ALSTAR2) is prospectively seeking functional and structural biomarkers at stages before the currently approved end point, that is, expansion of pre-existing atrophy.

In early AMD phases, visual acuity in bright light may be preserved, and prior histologic analysis[4,10] and

1

Investigative Ophthalmology & Visual Science

functional studies[11–15] support a greater vulnerability of rods than cones. Published data from ALSTAR2 baseline[10,15] reinforced two additional concepts apparent in previous studies with smaller samples.[16,17] First, a slowing of rod sensitivity recovery after a bright light (rod-mediated dark adaptation [RMDA]) was found to separate healthy eyes from eyes with intermediate AMD much better than eight other visual tasks, including steady state rod sensitivity, performed by the same patients. Second, as expected, RMDA was found to slow more markedly near the fovea (5 degrees) where rods are relatively sparse, than in the perifovea (12 degrees), where they are abundant. ALSTAR2 study design posits that dynamic changes in photoreceptor sustenance, represented by RMDA, and subserved by changes in the choriocapillaris-BrM-RPE complex, precedes loss of steady state sensitivity, represented by changes in outer segments. RMDA may be delayed directly by deposits blocking transfer of retinoids and other essentials, indirectly by reduced functionality of adjacent cells (e.g. loss of RPE apical processes involved in transfer),[18] or both. High-risk drusen cluster under the fovea and the inner ring of the Early Treatment of Diabetic Retinopathy Study (ETDRS) grid, mirroring foveal cones and their support cells. In contrast, subretinal drusenoid deposits (SDDs) appear first within the outer superior subfield of the ETDRS grid where rod photoreceptors are maximal and spread toward the fovea. Poorer rod vision near the fovea, as noted for years,[11,19] held even in eyes with SDDs.[17,20]

In early stages of AMD, drusen and RPE abnormalities are hallmark diagnostic and prognostic fundus features.[21–23] AMD staging systems use assessment of stereoscopic fundus photographs, with the Beckman and Age-Related Eye Disease Study (AREDS) 9-step scales[24,25] being commonly used. Although the AREDS system is more granular (9 vs. 5 steps), both involve assessment of drusen and pigmentary abnormalities in the 6-mm diameter ETDRS grid.[25] Neither system incorporates the recently recognized SDD (reticular pseudodrusen), stereotypic extracellular material between photoreceptors and the RPE. Optical coherence tomography (OCT) has transformed AMD diagnosis and management due to high axial resolution that reveals disease processes in specific tissue layers, including the extracellular deposits.[26,27] Thus, disease progression can be quantified by segmenting layer boundaries and computing thicknesses.[28]

In this report, we use a semi-automated approach to quantify thickness of outer retinal bands, in concentric rings of the ETDRS grid, in eyes with healthy, early AMD, and intermediate AMD, as defined by the AREDS and Beckman scales for the baseline visit of ALSTAR2. Our purpose was to seek structural changes in different stages of AMD in the context of a deposit-driven progression sequence model described above, specifically to determine at what AMD severity stage reflective bands attributable to photoreceptors and deposits were affected.

## METHODS AND MATERIALS

Subjects ages ≥ 60 years with healthy macular health, and eyes with early AMD, or intermediate AMD were enrolled in ALSTAR2. Details of the study protocol and baseline demographic characteristics have been described.[29,30] To ensure good fixation, one eye from each recruited patient, that is, the eye with better acuity, was chosen for the study. All subjects underwent complete eye examination, multimodal imaging (i.e. flash color fundus photographs [CFPs], fundus autofluorescence, volume OCT, and OCT angiogra-

phy). Patients with a history of intraocular surgery, glaucoma, optic neuritis, refractive error > 6 diopters, history of diabetes and diabetic retinopathy, vascular pathologies, such as retinal vein and artery occlusion, and a history of intraocular injection were excluded.

AMD presence and severity was determined using both the AREDS 9-step and Beckman classification schemes for CFP.[24,25] We used two systems because different investigators in the field use one or another, and we want our data to be useful to both. For the AREDS scale, normal macular health is step 1, early AMD spans are steps 2 to 4, and intermediate AMD spans are steps 5 to 8. The Beckman system includes normal aging (grades 1 and 2), early AMD (grade 3), and intermediate AMD (grade 4). One eye was selected as the study eye for functional testing and the OCT analysis of this report.

The study protocol was approved by institutional review boards of the University of Alabama at Birmingham and the University of California – Los Angeles. Research followed the principles of the Declaration of Helsinki.

## Optical Coherence Topography Acquisition and Grading

All OCT images were acquired by an experienced operator (author M.E.C.) using the Spectralis HRA + OCT2 (Heidelberg Engineering, Heidelberg, Germany). The field of view of the fovea-centered volume OCT scan was 30 degrees × 25 degrees (8.6 × 7.2 mm) and consisted of 121 horizontal B-scans × 512 A-scans with real time averaging of 9.[30] OCT volumes were exported and transferred to the Doheny Image Analysis Laboratory (DIAL) for automated segmentation. At the Doheny Image Reading and Research Laboratory (DIRRL), retinal layers were segmented with a deep-learning-derived algorithm, followed by manual correction/refinement.

Performance of the automated deep-learning-derived graph-based algorithm for multilayer segmentation has been described.[28] For this study, the algorithm segmented six outer retinal layers (defined by 7 surfaces; Fig. 1): photoreceptor inner segments (PISs; spanning from the centerlines of the external limiting membrane [ELM] to the ellipsoid zone [EZ] center line), photoreceptor outer segments (POSs; EZ center line to the inner surface of the SDD if present/interdigitation zone [IZ] center line if SDD absent; IZ defined as a hyper-reflective band between the EZ and the RPE), SDD (SDD inner surface –IZ center line), RPE + basal lamina (BL; IZ center line to the outer border of the RPE + BL band/inner drusen surface when drusen were present), drusen (drusen inner surface to the BrM), and choroid (BrM to the choroid-sclera junction).[28] In the absence of drusen, the outer border of the RPE + BL layer was defined as BrM. We use the term RPE + BL to indicate the RPE with or without basal laminar deposit, an acquired layer between the RPE plasma membrane and native basal lamina and a defining feature of AMD[31] (Supplementary Table 1).

Following automated segmentation, two trained DIRRL graders (authors S.F.A. and C.V.) inspected the boundary positions on all 121 B-scans and manually corrected segmentation errors using reading center OCT grading software (3D OCTOR) developed by DIAL and previously validated by the reading center.[28,32] Following verification of boundary positions, the 3D OCTOR software calculated thicknesses of six layers at each A-scan location and generated thickness maps (Fig. 2).[28] Thickness values were computed within
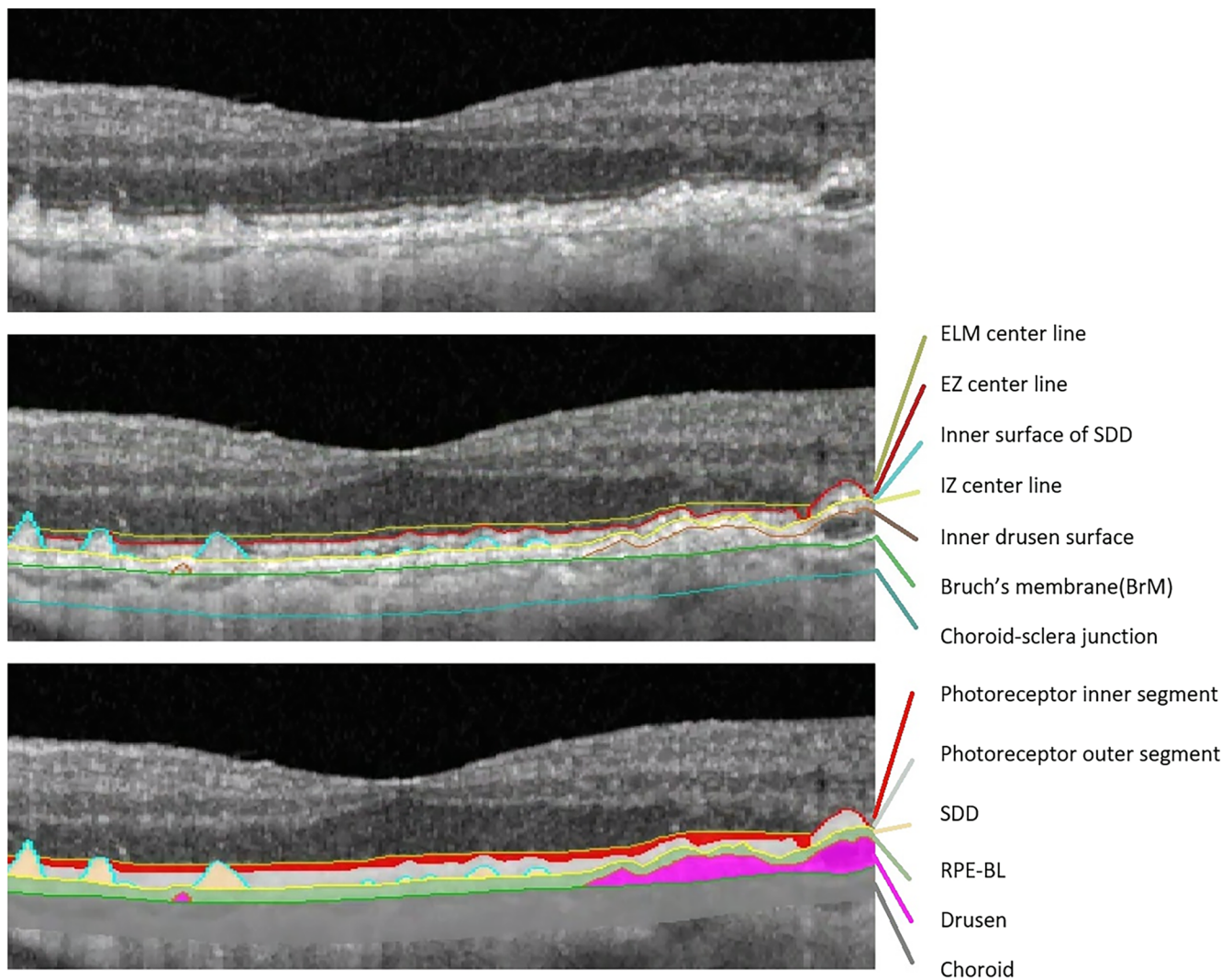
**FIGURE 1.** **Segmentation of bands in the central B-scan.** The *upper panel* shows an OCT B-scan the eye of a subject classified as having intermediate AMD by both the AREDS and Beckman scales in the central B-scan. The *middle panel* shows the seven surfaces used for segmenting the outer retinal and choroid layers. The *lower panel* shows the segmented layers. (ELM = external limiting membrane; EZ = ellipsoid zone; SDD = subretinal drusenoid deposit; IZ = interdigitation zone; RPE-BL = retinal pigment epithelium basal lamina).

each of the nine ETDRS subfields: superior outer (field 1); nasal outer (2); inferior outer (3); temporal outer (4); superior inner (5); nasal inner (6); inferior inner (7); temporal inner (8); central subfield (CSF; or field 9), as well as combinations including all nine subfields, and the inner and outer rings (subfields 5–8 and 1–4, respectively). For drusen and SDD, average thicknesses less than 0.01 are shown as zero. We emphasize thicknesses within the rings, because the distribution of cones and rods in the central human retina are roughly radially symmetric around the point of highest cone density. The distribution of high risk drusen and SDD are hypothesized dysregulations of constitutive intercellular transfer pathways specific to cone and rod photoreceptors.[33]

## Graphical Display of Thicknesses

To visualize differences among diagnostic groups (healthy, early AMD, intermediate AMD eyes), frequency distributions of mean thickness of each of the four retinal layers, for the entire ETDRS grid, were plotted for each group. Frequency distributions of SDD and drusen thicknesses were created by omitting the many eyes with zero thicknesses for these deposits. So that shifts in the distribution of thicknesses could be visualized separately from differences in group size, frequency distributions were normalized to the modal (most frequent) thickness for each group.

## Statistical Analysis of Thicknesses

Continuous variables were presented as means and standard deviations. Normality was assessed using the Kolmogorov-Smirnov test. Age differences between groups were analyzed using analysis of variance (ANOVA). To account for potential age differences, an analysis of covariance (ANCOVA) was performed with age included as a covariate. Post hoc tests with Bonferroni correction were conducted to identify specific group differences. To determine the impact of deposits on the thickness of photoreceptor inner and outer segments in healthy, early AMD, and intermediate AMD eyes, we stratified subjects into those with and without SDD and
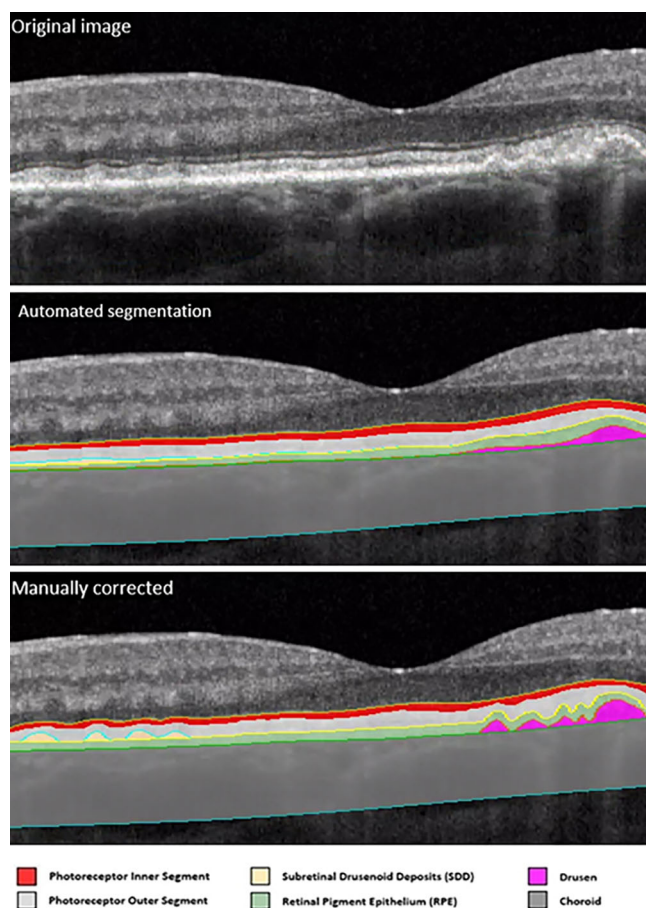
**FIGURE 2. Segmentation of bands in an OCT B-scan crossed the fovea.** The *upper panel* shows an OCT B-scan the eye of a subject classified as having intermediate AMD by both the AREDS and Beckman scales. The *middle panel* shows a shaded overlay of the outer retinal/choroidal layers following automated segmentation. The *lower panel* shows the segmented layers following manual correction of segmentation errors. Note, the drusen are taller and narrower following manual correction.

those with and without drusen. We conducted a similar analysis for choroidal thickness within these three diagnostic groups, comparing eyes with and without SDD. All statistical analyses were performed using SPSS software (IBM Corp. released 2017; IBM SPSS Statistics for Windows, version 27.0. Armonk, NY, USA). A significance level of $P < 0.05$ was used for all analyses.

## RESULTS

The ALSTAR2 baseline dataset included 502 eyes from 502 persons (203 men [40%] and 299 [60%] women). Under the AREDS classification, 252 eyes were deemed healthy aged, 147 had early AMD, and 103 had intermediate AMD (see Table 1). The average age was $70.9 \pm 5.8$ for healthy, $71.4 \pm 6.3$ for early AMD, and $74.3 \pm 5.5$ for intermediate AMD, with the latter group significantly older than the other 2 groups ($P < 0.001$). When the cohort was classified using the Beckman Scale, 242 eyes were graded as healthy aged, 98 as early AMD, and 162 as intermediate AMD (see Table 1). The average age was $70.7 \pm 5.8$ for healthy, $71.6 \pm 6.1$ for early AMD, and $73.3 \pm 6.0$ for intermediate AMD. The intermediate AMD group was significantly older than the healthy group ($P < 0.001$) but not the early AMD group.

The distributions of AMD stages using the AREDS and Beckman scales were compared (see Table 1). By both systems, 227, 70, and 100 eyes were considered healthy, having early AMD, and having intermediate AMD, respectively. Some eyes changed grades when assessed by the other system: 25 AREDS healthy eyes were Beckman early AMD, 15 AREDS early AMD eyes were Beckman healthy, and 3 AREDS intermediate AMD eyes were Beckman early (9.9%, 10.2%, and 2.9% of the respective AREDS groups). We consider these transpositions noise in the grading system. However, 62 AREDS early AMD eyes were intermediate AMD by Beckman scales. Thus, 42.2% of the patients classified as early AMD on the AREDS scale was considered intermediate AMD by the Beckman scale.

Thicknesses of 6 outer retinal and choroidal layers in the entire ETDRS grid, inner and outer rings, and the central subfield for healthy, early AMD, and intermediate AMD eyes are shown in Table 2 (AREDS) and Table 3 (Beckman). Thicknesses in individual subfields are available in Supplementary Tables 2 to 7.

For PIS stratified by the AREDS scale (see Table 2), there was no significant difference between normal aging and early AMD eyes. Intermediate AMD eyes demonstrated thinner PIS in the entire grid, CSF, inner ring, and outer ring, compared to normal aging eyes, and thinner PIS compared to early AMD eyes in the CSF.

POS in the entire EDTRS grid were thinner in early AMD eyes compared to normal eyes, as stratified by AREDS (see Table 2). Intermediate AMD eyes had thicker POS in both the inner ring and CSF compared to both healthy and early AMD eyes, and compared to early AMD eyes, across the whole grid.

For eyes stratified by AREDS (see Table 2), RPE + BL was thinner in intermediate AMD eyes compared to both normal and early AMD eyes for the entire grid, inner ring, and CSF. There was no difference between healthy eyes and early AMD eyes.

For eyes stratified by AREDS (see Table 2), mean thickness of drusen and SDD showed no significant difference between healthy eyes and early AMD eyes. However, a significant increase in thickness was observed between intermediate AMD eyes and both healthy and early AMD

**TABLE 1.** Comparison of AMD Classification of Eyes in the Baseline by AREDS 9-Step Scale and Beckman

| | *N* | Beckman Normal | Beckman Early | Beckman Intermediate |
|---|---|---|---|---|
| *N* | | 242 | 98 | 162 |
| AREDS normal | 252 | **227** | 25 | 0 |
| AREDS early | 147 | 15 | **70** | 62 |
| AREDS intermediate | 103 | 0 | 3 | **100** |

Statistically significant result are presented in bold.

**TABLE 2.** Mean Thickness of Photoreceptor Inner and Outer Segments, RPE, Drusen, Subretinal Drusenoid Deposit (SDD), and Choroid Among Normal, Early, and Intermediate (Int) AMD Eyes (Classified by the AREDS 9 Step Scale) for EDTRS Subfields

| Layers | | *N* Age, Y | Normal 252 70.9 ± 5.8 | Early AMD 147 71.4 ± 6.3 | Normal Versus Early *P* Value 0.66 | Int AMD 103 74.3 ± 5.5 | Norm Versus Int *P* Value <0.001 | Early Versus Int *P* Value <0.001 |
|---|---|---|---|---|---|---|---|---|
| Mean thickness, µm | | | | | | | | |
| Photoreceptor inner | Entire EDTRS | | 16.2 ± 0.09 | 15.9 ± 0.12 | 0.11 | 15.6 ± 0.15 | **0.001** | 0.08 |
| segments | Outer ring | | 15.4 ± 0.09 | 15.2 ± 0.12 | 0.49 | 14.9 ± 0.14 | **0.01** | 0.39 |
| | Inner ring | | 18.4 ± 0.12 | 18.0 ± 0.15 | 0.22 | 17.6 ± 0.19 | **<0.001** | 0.19 |
| | Central subfield | | 20.6 ± 0.16 | 20.3 ± 0.21 | 0.67 | 19.4 ± 0.26 | **<0.001** | **0.04** |
| Photoreceptor outer | Entire EDTRS | | 29.4 ± 0.21 | 28.7 ± 0.28 | **0.04** | 29.8 ± 0.34 | 0.32 | **0.01** |
| segments | Outer ring | | 29.4 ± 0.22 | 28.5 ± 0.29 | 0.07 | 29.2 ± 0.35 | 0.46 | 0.39 |
| | Inner ring | | 29.4 ± 0.21 | 29.0 ± 0.27 | 0.71 | 31.3 ± 0.33 | **<0.001** | **<0.001** |
| | Central subfield | | 31.0 ± 0.26 | 31.0 ± 0.35 | 0.54 | 33.9 ± 0.42 | **<0.001** | **<0.001** |
| RPE + BL | Entire EDTRS | | 34.3 ± 0.16 | 34.6 ± 0.20 | 0.33 | 33.2 ± 0.25 | **<0.001** | **<0.001** |
| | Outer ring | | 33.9 ± 0.16 | 34.3 ± 0.21 | 0.41 | 33.2 ± 0.26 | 0.08 | **0.004** |
| | Inner ring | | 35.7 ± 0.16 | 35.6 ± 0.21 | 0.31 | 33.4 ± 0.26 | **<0.001** | **<0.001** |
| | Central subfield | | 36.2 ± 0.20 | 35.6 ± 0.26 | 0.21 | 33.3 ± 0.31 | **<0.001** | **<0.001** |
| Drusen | Entire EDTRS | | 0.0 ± 0.06 | 0.0 ± 0.07 | 0.9 | 1.6 ± 0.09 | **<0.001** | **<0.001** |
| | Outer ring | | 0.0 ± 0.03 | 0.0 ± 0.03 | 0.92 | 0.7 ± 0.04 | **<0.001** | **<0.001** |
| | Inner ring | | 0.0 ± 0.16 | 0.0 ± 0.21 | 0.86 | 4.1 ± 0.26 | **<0.001** | **<0.001** |
| | Central subfield | | 0.0 ± 0.33 | 0.0 ± 0.29 | 0.88 | 7.5 ± 0.53 | **<0.001** | **<0.001** |
| Subretinal drusenoid | Entire EDTRS | | 0.0 ± 0.01 | 0.0 ± 0.01 | 0.34 | 0.1 ± 0.01 | **<0.001** | **<0.001** |
| deposit (SDD) | Outer ring | | 0.0 ± 0.01 | 0.0 ± 0.01 | 0.99 | 0.1 ± 0.02 | **<0.001** | **<0.001** |
| | Inner ring | | 0.0 ± 0.01 | 0.0 ± 0.01 | 0.87 | 0.2 ± 0.02 | **<0.001** | **<0.001** |
| | Central subfield | | 0.0 ± 0.01 | 0.0 ± 0.02 | 0.83 | 0.2 ± 0.02 | **<0.001** | **<0.001** |
| Choroid | Entire EDTRS | | 177.8 ± 2.84 | 187.1 ± 3.71 | **0.04** | 171.4 ± 4.52 | 0.24 | **0.008** |
| | Outer ring | | 174.5 ± 2.78 | 183.9 ± 3.62 | 0.24 | 169.0 ± 4.41 | 0.38 | **0.01** |
| | Inner ring | | 187.4 ± 3.10 | 196.3 ± 4.04 | 0.11 | 178.5 ± 4.93 | 0.91 | **0.02** |
| | Central subfield | | 190.4 ± 3.33 | 199.5 ± 4.34 | 0.29 | 179.8 ± 5.29 | 0.27 | **0.01** |

Statistically significant result are presented in bold.

eyes, for the entire grid, outer and inner rings, and CSF.

It is shown that 10% of healthy, 25% of early AMD, and 94% of intermediate AMD of eyes classified by the AREDS scale, have measurable drusen in at least one ETDRS subfield, as do 9% of healthy, 30% of early AMD, and 67% of intermediate AMD classified by Beckman. In addition, 10% of healthy eyes, 25% of early AMD eyes, and 32% of intermediate AMD of eyes classified by the AREDS scale, have measurable SDD in at least one EDTRS subfield, and 9% of healthy, 27% of early AMD, and 44% of intermediate AMD eyes have measurable SDD when stratified by the Beckman scale.

For eyes stratified by AREDS (see Table 2), the choroid was thinner in intermediate AMD eyes compared to early AMD eyes for the entire grid, inner and outer rings, and the CSF. For the entire grid only, early AMD eyes also showed a thicker choroid compared to normal eyes.

Thicknesses for eyes stratified by the Beckman scale (see Table 3) can be referenced to thicknesses from eyes stratified by the AREDS scale (Table 2). Some significant differences among AREDS-stratified groups were no longer significant among Beckman-stratified groups, as indicated by highlighting in Table 3. Of note, the comparison of healthy versus early AMD eyes became nonsignificant for PIS and the choroid. The comparison between intermediate AMD and both healthy and early AMD became insignificant for the choroid as well. However, major patterns remained clear regardless of the grading system. The most consistent significant differences between severity groups were found for the acquired layers of drusen and SDD

(entire grid, outer ring, inner ring, and CSF), followed by RPE + BL (entire grid, inner ring, and CSF). Less consistent differences were found for PIS and POS. Choroidal thickness showed no consistent relationship with AMD severity.

Distributions of thicknesses of outer retinal bands and choroid in the whole ETDRS grid of AREDS-stratified eyes are shown graphically in Figure 3. Relative to healthy eyes, PIS thin slightly in intermediate AMD, POS stay the same or thicken slightly in intermediate AMD, RPE is thinner in intermediate AMD, and choroidal thickness does not show a consistent relationship among groups. Distributions of nonzero thicknesses of the acquired layers of SDD and drusen are shown in Figure 4. For both SDD and drusen, there is an extended positive-going tail of thicknesses in intermediate AMD eyes only.

In the stratified analysis of healthy, early AMD, and intermediate AMD groups, no significant differences in PIS and POS were observed between eyes with and without SDD or between eyes with and without drusen. The results remained consistent, indicating that the presence of SDD and drusen did not significantly influence photoreceptor thickness in the studied population. Additionally, we did not observe any significant differences in choroidal thickness between eyes with and without SDD.

## DISCUSSION

This study is notable for determining many chorioretinal thicknesses for a large cohort of eyes, including many

**TABLE 3.** Mean Thickness of the Photoreceptor Inner and Outer Segments, RPE, Drusen, Subretinal Drusenoid Deposit (SDD), and Choroid Among Normal, Early, and Intermediate (Int) AMD Eyes (Classified by the Beckman Scale) for EDTRS Subfields

| Layers | N Age, Y | Normal 242 70.7 ± 5.8 | Early AMD 98 71.7 ± 6.2 | Norm Versus Early P Value 0.38 | Int AMD P Value 73.4 ± 6.1 | Norm Versus Int 103 <0.001 | Early Versus Int P Value 0.07 |
|---|---|---|---|---|---|---|---|
| Mean thickness (µm) | | | | | | | |
| Photoreceptor inner segments | Entire EDTRS | 16.2 ± 0.09 | 16.0 ± 0.15 | 0.28 | 15.7 ± 0.12 | **0.004** | 0.19 |
| | Outer ring | 15.4 ± 0.09 | 15.2 ± 0.14 | 0.97 | 15.0 ± 0.11 | **0.02** | 0.63 |
| | Inner ring | 18.4 ± 0.12 | 18.1 ± 0.19 | 0.77 | 17.8 ± 0.15 | **0.01** | 0.57 |
| | Central subfield | 20.6 ± 0.17 | 20.1 ± 0.26 | 0.38 | 19.8 ± 0.20 | **0.02** | 0.65* |
| Photoreceptor outer segments | Entire EDTRS | 29.4 ± 0.22 | 28.7 ± 0.34 | 0.10* | 29.4 ± 0.27 | 0.88 | 0.10* |
| | Outer ring | 29.3 ± 0.23 | 28.6 ± 0.36 | 0.24 | 29.0 ± 0.28 | 0.78 | 0.39 |
| | Inner ring | 29.4 ± 0.22 | 28.9 ± 0.34 | 0.78 | 30.5 ± 0.27 | **0.004** | **<0.001** |
| | Central subfield | 31.0 ± 0.27 | 30.9 ± 0.43 | 0.67 | 33.0 ± 0.34 | **<0.001** | **<0.001** |
| RPE +BL | Entire EDTRS | 34.5 ± 0.25 | 34.5 ± 0.25 | 0.51 | 33.7 ± 0.20 | **0.02** | **0.01** |
| | Outer ring | 33.9 ± 0.17 | 34.2 ± 0.26 | 0.95 | 33.6 ± 0.21 | 0.94 | 0.24* |
| | Inner ring | 35.7 ± 0.17 | 35.6 ± 0.26 | 0.56 | 34.2 ± 0.21 | **<0.001** | **<0.001** |
| | Central subfield | 36.2 ± 0.20 | 35.6 ± 0.32 | 0.33 | 34.2 ± 0.25 | **<0.001** | **0.003** |
| Drusen | Entire EDTRS | 0.0 ± 0.06 | 0.0 ± 0.10 | 0.96 | 1.0 ± 0.08 | **<0.001** | **<0.001** |
| | Outer ring | 0.0 ± 0.03 | 0.0 ± 0.04 | 0.87 | 0.4 ± 0.03 | **<0.001** | **<0.001** |
| | Inner ring | 0.1 ± 0.18 | 0.1 ± 0.28 | 0.88 | 2.6 ± 0.22 | **<0.001** | **<0.001** |
| | Central subfield | 0.1 ± 0.36 | 0.1 ± 0.57 | 0.65 | 4.7 ± 0.45 | **<0.001** | **<0.001** |
| Subretinal drusenoid deposit (SDD) | Entire EDTRS | 0.0 ± 0.01 | 0.0 ± 0.02 | 0.9 | 0.1 ± 0.01 | **<0.001** | **<0.001** |
| | Outer ring | 0.0 ± 0.01 | 0.0 ± 0.02 | 0.78 | 0.1 ± 0.01 | **<0.001** | **<0.001** |
| | Inner ring | 0.0 ± 0.01 | 0.0 ± 0.02 | 0.91 | 0.1 ± 0.01 | **<0.001** | **<0.001** |
| | Central subfield | 0.0 ± 0.01 | 0.0 ± 0.02 | 0.69 | 0.1 ± 0.02 | **<0.001** | **0.01** |
| Choroid | Entire EDTRS | 178.0 ± 2.93 | 180.9 ± 4.57 | 0.59* | 179.9 ± 3.6 | 0.69 | 0.85* |
| | Outer ring | 174.7 ± 2.86 | 178.0 ± 4.46 | 0.34 | 177.1 ± 3.51 | 0.54 | 0.69* |
| | Inner ring | 187.9 ± 3.20 | 189.6 ± 4.99 | 0.64 | 187.8 ± 3.93 | 0.62 | 0.78* |
| | Central subfield | 190.7 ± 3.43 | 192.7 ± 5.36 | 0.15 | 190.0 ± 4.21 | 0.37 | 0.52* |

\* Some significant differences among AREDS-stratified groups were no longer significant among Beckman-stratified groups (Table 2), as highlighted and marked by an asterisk (*).

normal aged eyes, all previously characterized for performance on visual tasks over a range of retinal illuminance. Regardless of the AMD classification system used, we found no significant difference between healthy and early AMD eyes in the mean thickness of inner segments, RPE, drusen, and SDD. We found significant and consistent differences in intermediate AMD eyes, compared to early AMD and healthy eyes, with generally thinner inner segments and RPE and thicker drusen and SDD. Outer segments were thinner in early AMD eyes than either healthy or intermediate AMD eyes. The most consistent difference, across all spatial assessments, was the greater amount of drusen and SDD, especially in intermediate AMD eyes.

The limited evidence for structural changes in photoreceptor- and RPE-attributable bands between healthy and early AMD is surprising given the strong functional findings in the ALSTAR2 baseline cohort.[16,17] The current results are consistent with our hypothesis (but cannot prove it) that changes in dynamic photoreceptor sustenance, represented by RMDA and subserved by the choriocapillaris-BrM-RPE complex, would precede loss of steady state sensitivity, represented by changes in the outer segment structure. A salient functional finding for the ALSTAR2 baseline cohort was a robust difference between normal aging and early AMD for RMDA and not for scotopic sensitivity assessed at the same location,[16] and thus structural differences between those stages, as explored in the current study, are of interest. OCT assessments such as ours are valuable because of the limited availability of relevant histologic data. It is difficult to obtain in post-mortem eyes at early stages of AMD that are attached over a sufficiently wide area for meaningful quantitative measures of outer segment integrity. Photoreceptor shortening over individual drusen or SDD can be seen in retinal samples that remain attached.[33,34]

Outer segments in the entire ETDRS grid appeared thinner, only at early AMD, and only when eyes were assessed by the AREDS system. The non-progressive differences in POS thickness could represent an artifact of measurement technique, a complex relationship of POS with bands on either side of it, or changes in the outer segments themselves. Regarding measurement technique, our segmentation approach identified specific surfaces/boundaries, and outer segments were defined to span between the EZ centerline and the IZ centerline (or surface of SDD if present). It is possible that photoreceptor debris or early SDD that could not be resolved from the IZ may have been included in POS measurements in eyes with intermediate AMD. Regarding impact of neighboring structures, our data also show that PIS and RPE were thinner with greater AMD severity. RPE thicknesses included both the cell body (in the RPE-basal lamina-BrM band) and apical processes (in the IZ). There is little histologic evidence for thinning of the RPE cell body at non-atrophic areas of AMD eyes.[31] Further, other analyses of this OCT dataset indicates disintegrity of the IZ in early and intermediate AMD.[35] Thus, one possible explanation of the current POS results is that IZ disintegrity and shortening of inner segments (thus pulling up outer segments away from the RPE cell bodies) together resulted
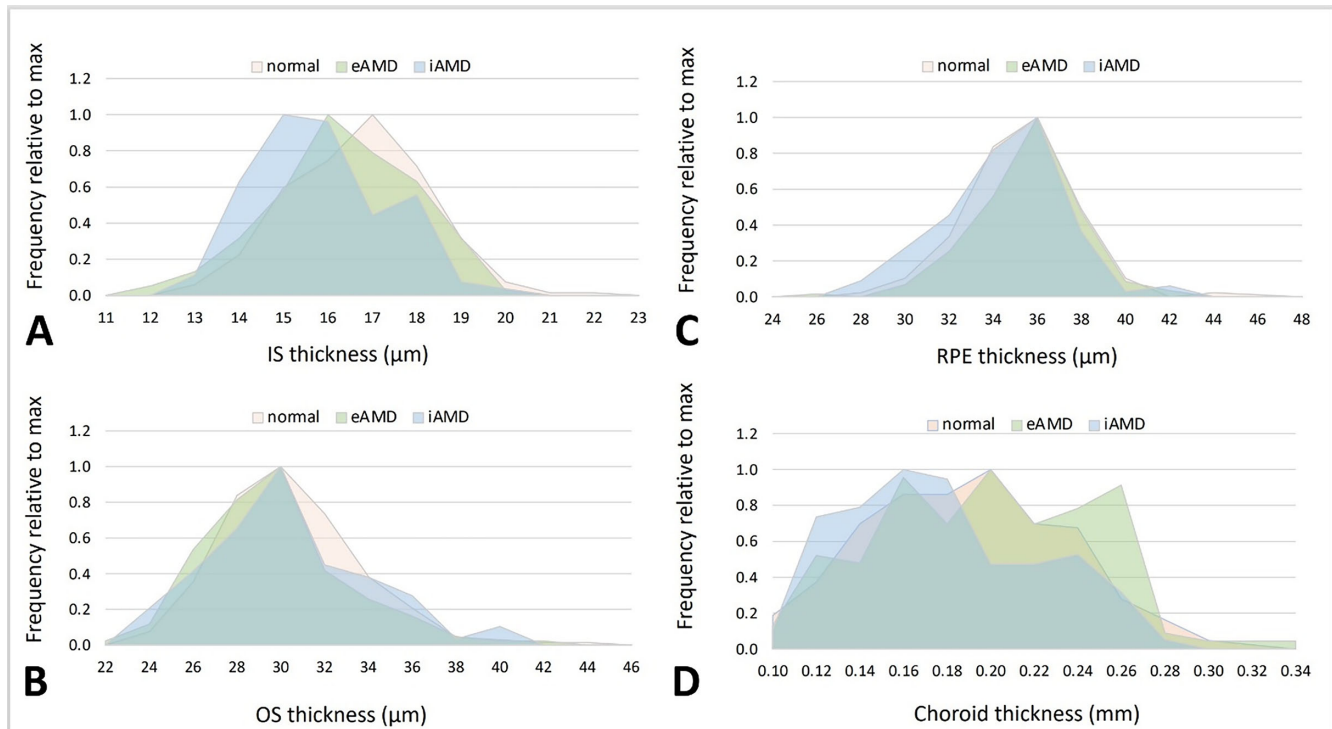
**FIGURE 3.** **Distribution of mean thicknesses of outer retinal bands and choroid.** Area plot of mean thickness across the ETDRS grid shows the frequency of eyes at each thickness, plotted relative to the modal (most frequent) thickness observed for each diagnostic group (healthy, early AMD = eAMD, intermediate AMD = iAMD). (**A**) Inner segments are slightly thicker in healthy eyes. (**B**) Outer segments are thicker in iAMD eyes than in the other groups. (**C**) RPE is thinner in iAMD eyes. (**D**) Choroidal thickness does not show a consistent relationship among groups.

in inclusion of more bared outer segments in POS thickness measurements.

Our data showing that RPE-BL thins, primarily centrally, from healthy eyes to intermediate AMD eyes cannot be readily compared to previous studies due to methodologic considerations. In our study, the RPE-BL band included the IZ up to its centerline, and a modal thickness of 36 μm was reported (see Fig. 3). The IZ was the last of four major outer retinal hyper-reflective bands to be recognized, with the introduction of spectral domain OCT. The 2014 clinical consensus[36] adopted IZ terminology, based on published histology showing photoreceptor outer segments and RPE apical processes internal to RPE cell bodies. An OCT study by Karampelas et al. reported that RPE/BrM, also including some portion of IZ but thinner than our values, was significantly thicker in dry AMD than in healthy eyes.[37] Whether this thickening appeared in early versus intermediate AMD eyes was not investigated. Brandl and colleagues analyzed 822 eyes and showed that the RPE/BrM complex was thicker in early AMD eyes compared to eyes without AMD.[38] However, they did not include the IZ, reporting smaller thicknesses (13.8-16.6 μm) consistent with RPE cell bodies alone.[39] Further, they subdivided early AMD into three stages, and found that thickening was observed in the latter stages only. Finally, Trinh and colleagues used spectral domain OCT in healthy eyes, early eyes, and intermediate AMD eyes (*N* = 96, 48, and 48, respectively), and observed greater thinning of the RPE-BL-BrM band with increasing eccentricity; these authors reported correlations but not measured thicknesses.[40] These differences between our studies and others highlight the need for

standardized terminology and methodology for comparability of data: such a system has been offered.[41] Ideally, a standard system would also respect the layering of cells, which does not necessarily conform to the layering of reflectivity.

A consistent effect across all ETDRS zones was the accumulation of extracellular deposits, especially in intermediate AMD. We did not observe significant differences in drusen thickness between normal healthy eyes (which can have small drusen ≤ 63 μm) and early AMD (which can have many small drusen and/or some medium drusen ≤ 125 μm) in our cohort. Eyes with intermediate AMD, however, have many medium drusen or at least one large druse (>250 μm), and thus can contribute substantially to a larger mean drusen thickness, as observed in the current and prior reports.[22,42] Drusen are the hallmark AMD lesion. They accumulate between the RPE-BL and the inner collagenous layer of BrM.[43–47] These were found in all analyzed ETDRS zones. Small drusen observed as RPE elevations on OCT may not contribute appreciably to mean drusen thickness or volume. In contrast to drusen, SDD accumulate between the photoreceptor outer segments and the apical surface of the RPE. The origin of this material remains under investigation, and a leading hypothesis is that SDD represents dysregulation of constitutive lipid transport across the subretinal space.[48–50] Over half of the persons with early to intermediate AMD and one-quarter of elderly people with healthy maculae have SDD.[51–54] SDD in healthy eyes and those with early AMD are typically smaller, and fewer in number than those in eyes with intermediate AMD.[21] Accordingly, SDD thickness was significantly greater in all subfields in intermedi-
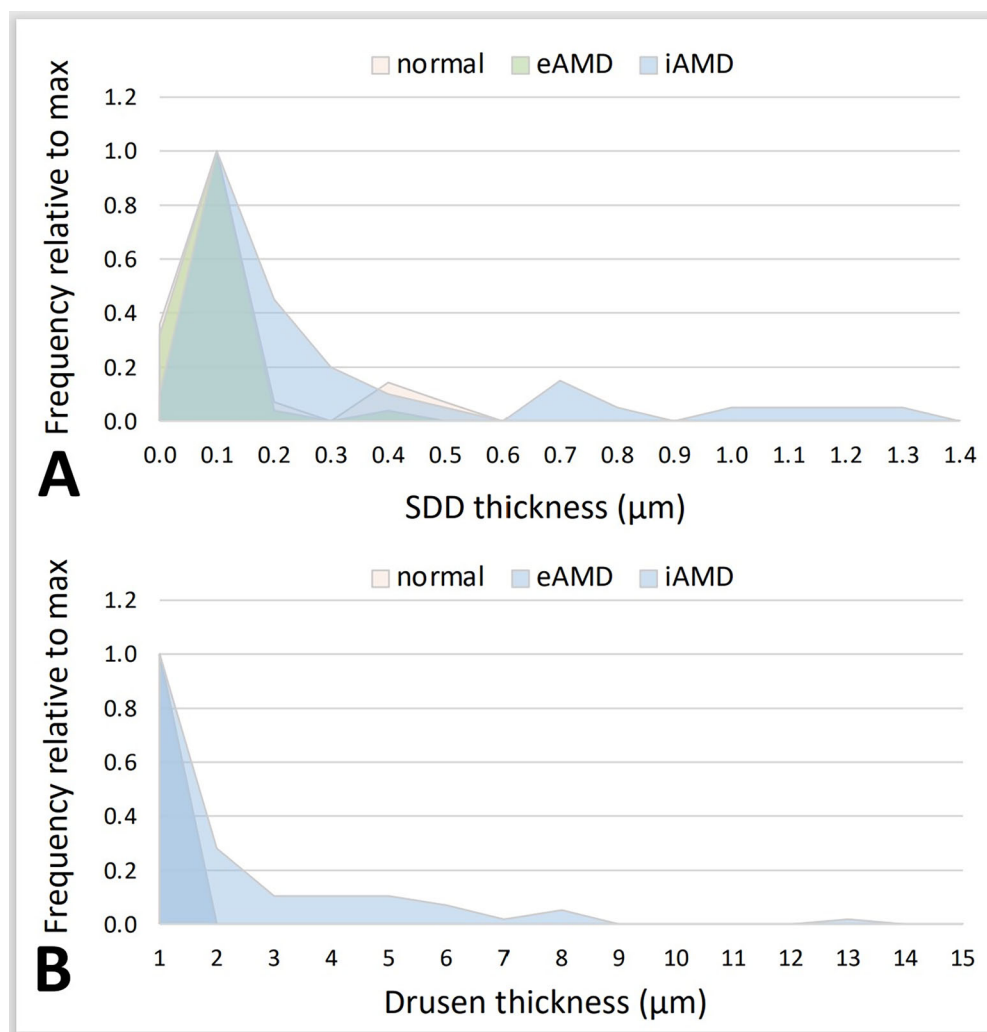
**FIGURE 4. Distribution of mean thicknesses of SDD and drusen bands.** Area plot of mean thickness across the ETDRS grid shows the frequency of eyes at each thickness, plotted relative to the maximum thickness observed for each diagnostic group (healthy, early AMD = eAMD, intermediate AMD = iAMD). For SDD (*top*) there is a mode of thickness at 0.1 µm for all groups and an extended positive-going tail of thicknesses in intermediate AMD eyes only. For drusen, there is a mode of thicknesses at 1 µm for all groups and an extended positive-going tail of thicknesses in intermediate AMD eyes only.

ate AMD eyes in our study compared to healthy and early AMD eyes.

We observed a criterion-dependent difference in choroidal thickness (thicker choroid in early AMD and thinner in intermediate eyes by AREDS, no difference by the Beckman scale). In some studies, the choroid is thicker in early and intermediate AMD,[55–57] whereas others demonstrated significant choroidal thinning.[58–60] Multiple reports have failed to show that choroidal thickness significantly changes in AMD.[61,62] Arnold et al., showed that the presence of SDD is associated with choroidal fibrosis and thinning in eyes with SDD, however, most of the eyes in their studies were at a later stage of AMD than encountered in our study.[63] Based on the mentioned study, we used a stratified analysis and found no significant difference in choroidal thickness between eyes with and without SDD. Inconsistent results from published studies suggest that choroidal thickness may not show a specific relationship with AMD stage and may instead be influenced by factors such as smoking, age, and associated pachychoroid spectrum disor-

ders.[64] Other measures of choroidal health may be more informative, for example, choroidal vascular index, and the proportion of thickness occupied by vessels. However, histology has long showed,[65–68] and recent OCT angiography is now supporting,[69,70] that the degeneration of the choriocapillary microvasculature is a consistent feature of AMD progression and may possibly precede other changes. Reduced choriocapillaris flow signal has been linked to poorer visual function, including RMDA in the ALSTAR2 baseline cohort.[70,71] Further, the appearance of soft drusen can be explained in a straightforward manner if the initial step is impaired transport across the choriocapillaris-BrM interface. Using our current analysis methods for structural OCT, it is not feasible to reliably assess choriocapillaris thickness.

We found that two effects typically associated with AMD severity (thinning of POS and choroid) were significant when eyes were stratified by the AREDS scale but not when the same eyes were stratified by the Beckman scale. As evident in Table 1, a significant proportion (42%) of patients

classified as early AMD by the AREDS scale were classified as intermediate AMD by the Beckman scale. We attribute this switch to the Beckman scale classifying an eye with pigmentary abnormalities with or without drusen as intermediate AMD. This subgroup of early AMD (by AREDS) may merit separate analyses of functional characteristics in the future. The AREDS and Beckman scales were developed for different purposes (progression risk and clinical consensus, respectively). Although our findings were similar for many metrics regardless of the AMD classification system used, the different results for POS and choroid highlight the need for a consistent and validated classification system for AMD severity, especially at the earliest stage, before secondary effects and complications.

Strengths of our study include data from a large cohort with a standardized imaging protocol, comparison of two different AMD classification systems, use of the ETDRS grid to capture effects relevant to photoreceptor topography, and a robust protocol including trained reading center graders manually inspecting and correcting B-scan following automatic segmentation by a deep learning algorithm. Our study also has limitations. Segmentation and thickness assessments were limited by the axial resolution of our OCT device,[72] which is nominally approximately 6 to 7 μm. Some of the measured bands, such as PIS, are only 15 to 20 μm in thickness. Even though we measured between the centers of bright bands on OCT to ensure accurate thickness measurements, precision was ultimately limited by the device. Future directions should include a uniform AMD classification system to solve these kinds of differences between various classification scales. In addition, future studies using high-resolution (2 μm) OCT may prove informative.[72]

## CONCLUSIONS

Our study found no significant changes in the thickness of outer retinal and choroidal layers between normal aging and early AMD, except thinning of photoreceptor outer segments in early AMD eyes, and only when classified on the AREDS scale. This observation suggests that functional alterations, especially slowing of RMDA, may precede structural changes in early AMD eyes as detected by widely used current spectral domain OCT technology. Analysis of other imaging technologies in the ongoing prospective observational trial will reveal additional structure-function correlations of interest.

Disclosure: **M. Emamverdi**, None; **C. Vatanatham**, None; **S. Fasih-Ahmad**, None; **Z. Wang**, None; **Z. Mishra**, None; **A. Jain**, None; **A. Ganegoda**, None; **M.E. Clark**, None; **A. Habibi**, None; **M. Ashrafkhorasani**, None; **C. Owsley**, Johnson & Johnson Vision (F); **C.A. Curcio**, Genentech/Hoffman LaRoche (F), Regeneron (F), Heidelberg Engineering (C, F, R); Apellis (C), Astellas (C), Boehringer Ingelheim (C), Character Biosciences (C), Osanni (C), and Annexon (outside this project); **Z.J. Hu**, Heidelberg Engineering (C, F, R); **S.R. Sadda**, 4DMT (C), AbbVie (C), Alexion (C), Allergan Inc. (C), Alnylam Pharmaceuticals (C), Amgen Inc. (C), Apellis Pharmaceuticals Inc. (C), Astellas (C), Bayer Healthcare Pharmaceuticals (C), Biogen MA Inc. (C), Boehringer Ingelheim (C), Catalyst Pharmaceuticals Inc. (C), Centervue Inc. (C, F), GENENTECH (C), Gyroscope Therapeutics (C), Hoffman La Roche Ltd. (C), Iveric Bio (C), Janssen Pharmaceuticals Inc. (C), Merck & Co. Inc. (C), Nanoscope (C), Notal Vision Inc. (C), Optos Inc. (C, F), Oxurion/Thrombogenics (C), Oyster Point Pharma (C), Pfizer Inc. (C), Regeneron Pharmaceuticals Inc. (C), Samsung Bioepis (C), Vertex Pharmaceuticals Incorporated (C), Carl Zeiss Meditec (C, F, R), Heidelberg Engineering (C, F, R), Novartis Pharma AG (C, R), Nidek Incorporated (F, R); Topcon Medical Systems Inc. (C, F, R)

## *References*

1. Lim LS, Mitchell P, Seddon JM, Holz FG, Wong TY. Age-related macular degeneration. *Lancet*. 2012;379(9827): 1728–1738.
2. Mitchell P, Liew G, Gopinath B, Wong TY. Age-related macular degeneration. *Lancet*. 2018;392(10153):1147–1159.
3. Wong WL, Su X, Li X, et al. Global prevalence of age-related macular degeneration and disease burden projection for 2020 and 2040: a systematic review and meta-analysis. *Lancet Glob Health*. 2014;2(2):e106–e116.
4. Curcio CA, Medeiros NE, Millican CL. Photoreceptor loss in age-related macular degeneration. *Invest Ophthalmol Vis Sci*. 1996;37(7):1236–1249.
5. Jackson GR, Owsley C, Curcio CA. Photoreceptor degeneration and dysfunction in aging and age-related maculopathy. *Ageing Res Rev*. 2002;1(3):381–396.
6. Medeiros NE, Curcio CA. Preservation of ganglion cell layer neurons in age-related macular degeneration. *Invest Ophthalmol Vis Sci*. 2001;42(3):795–803.
7. Emamverdi M, Habibi A, Ashrafkhorasani M, Nittala MG, Kadomoto S, Sadda SR. Optical coherence tomography features of macular hyperpigmented lesions without intraretinal hyperreflective foci in age-related macular degeneration. *Curr Eye Res*. 2023;49:1–7.
8. Curcio CA. Soft drusen in age-related macular degeneration: biology and targeting via the oil spill strategies. *Invest Ophthalmol Vis Sci*. 2018;59(4):AMD160–AMD181.
9. Curcio CA. Antecedents of soft drusen, the specific deposits of age-related macular degeneration, in the biology of human macula. *Invest Ophthalmol Vis Sci*. 2018;59(4):AMD182–AMD194.
10. Curcio C, Millican CL, Allen K, Kalina R. Aging of the human photoreceptor mosaic: evidence for selective vulnerability of rods in central retina. *Invest Ophthalmol Vis Sci*. 1993;34(12):3278–3296.
11. Owsley C, Jackson GR, Cideciyan AV, et al. Psychophysical evidence for rod vulnerability in age-related macular degeneration. *Invest Ophthalmol Vis Sci*. 2000;41(1):267–273.
12. Tahir HJ, Rodrigo-Diaz E, Parry NR, Kelly JM, Carden D, Murray IJ. Slowed dark adaptation in older eyes; effect of location. *Exp Eye Res*. 2017;155:47–53.
13. Tan RS, Guymer RH, Aung K-Z, Caruso E, Luu CD. Longitudinal assessment of rod function in intermediate age-related macular degeneration with and without reticular pseudodrusen. *Invest Ophthalmol Vis Sci*. 2019;60(5):1511–1518.
14. Flynn OJ, Cukras CA, Jeffrey BG. Characterization of rod function phenotypes across a range of age-related macular degeneration severities and subretinal drusenoid deposits. *Invest Ophthalmol Vis Sci*. 2018;59(6):2411–2421.
15. Binns AM, Taylor DJ, Edwards LA, Crabb DP. Determining optimal test parameters for assessing dark adaptation in people with intermediate age-related macular degeneration. *Invest Ophthalmol Vis Sci*. 2018;59(4):AMD114–AMD121.
16. Owsley C, Swain TA, McGwin G, et al. How vision is impaired from aging to early and intermediate age-related macular degeneration: insights from ALSTAR2 baseline. *Transl Vis Sci Technol*. 2022;11(7):17.

17. Owsley C, Swain TA, McGwin G, Jr, Clark ME, Kar D, Curcio CA. Biologically guided optimization of test target location for rod-mediated dark adaptation in age-related macular degeneration: Alabama Study on Early Age-related Macular Degeneration 2 Baseline. *Ophthalmol Sci*. 2023;3(2): 100274.

18. Berlin A, Matney E, Jones SG, et al. Discernibility of the interdigitation zone (IZ), a potential optical coherence tomography (OCT) biomarker for visual dysfunction in aging. *Curr Eye Res*. 2023;48(11):1050–1056.

19. Haimovici R, Owens SL, Fitzke FW, Bird AC. Dark adaptation in age-related macular degeneration: relationship to the fellow eye. *Graefes Arch Clin Exp Ophthalmol*. 2002;240:90–95.

20. Guymer RH, Tan RS, Luu CD. Comparison of visual function tests in intermediate age-related macular degeneration. *Transl Vis Sci Technol*. 2021;10(12):14.

21. Chen L, Messinger JD, Zhang Y, Spaide RF, Freund KB, Curcio CA. Subretinal drusenoid deposit in age-related macular degeneration: histologic insights into initiation, progression to atrophy, and imaging. *Retina (Philadelphia, Pa)*. 2020;40(4):618.

22. Spaide RF, Ooto S, Curcio CA. Subretinal drusenoid deposits AKA pseudodrusen. *Surv Ophthalmol*. 2018;63(6):782–815.

23. Emamverdi M, Habibi A, Ashrafkhorasani M, Nittala MG, Kadomoto S, Sadda SR. Optical coherence tomography features of macular hyperpigmented lesions without intraretinal hyperreflective foci in age-related macular degeneration. *Curr Eye Res*. 2024;49(1):73–79.

24. Davis MD, Gangnon RE, Lee LY, et al. The Age-Related Eye Disease Study severity scale for age-related macular degeneration: AREDS report No. 17. *Arch Ophthalmol (Chicago, Ill: 1960)*. 2005;123(11):1484–1498.

25. Ferris FL, III, Wilkinson C, Bird A, et al. Clinical classification of age-related macular degeneration. *Ophthalmology*. 2013;120(4):844–851.

26. Drexler W, Fujimoto JG. State-of-the-art retinal optical coherence tomography. *Prog Retin Eye Res*. 2008;27(1):45–88.

27. Savastano MC, Minnella AM, Tamburrino A, Giovinco G, Ventre S, Falsini B. Differential vulnerability of retinal layers to early age-related macular degeneration: evidence by SD-OCT segmentation analysis. *Invest Ophthalmol Vis Sci*. 2014;55(1):560–566.

28. Mishra Z, Ganegoda A, Selicha J, Wang Z, Sadda SR, Hu Z. Automated retinal layer segmentation using graph-based algorithm incorporating deep-learning-derived information. *Sci Rep*. 2020;10(1):9541.

29. An L, Wirth U, Koch D, et al. Metabolic role of autophagy in the pathogenesis and development of NAFLD. *Metabolites*. 2023;13(1):101.

30. Curcio CA, McGwin G, Sadda SR, et al. Functionally validated imaging endpoints in the Alabama study on early age-related macular degeneration 2 (ALSTAR2): design and methods. *BMC Ophthalmol*. 2020;20(1):1–17.

31. Sura AA, Chen L, Messinger JD, et al. Measuring the contributions of basal laminar deposit and Bruch's membrane in age-related macular degeneration. *Invest Ophthalmol Vis Sci*. 2020;61(13):19.

32. Schließleder G, Kalitzeos A, Kasilian M, et al. Deep phenotyping of PROM1-associated retinal degeneration. *Br J Ophthalmol*. 2023;108:558–565.

33. Curcio CA, Messinger JD, Sloan KR, McGwin G, Medeiros NE, Spaide RF. Subretinal drusenoid deposits in non-neovascular age-related macular degeneration: morphology, prevalence, topography, and biogenesis model. *Retina (Philadelphia, Pa)*. 2013;33(2):265–276.

34. Johnson PT, Lewis GP, Talaga KC, et al. Drusen-associated degeneration in the retina. *Invest Ophthalmol Vis Sci*. 2003;44(10):4481–4488.

35. Fasih-Ahmad S, Wang Z, Mishra Z, et al. Potential structural biomarkers in 3D images validated by the first functional biomarker for early age-related macular degeneration – ALSTAR2 Baseline. *Invest Ophthalmol Vis Sci*. 2024;65(2):1.

36. Staurenghi G, Sadda S, Chakravarthy U, Spaide RF. Proposed lexicon for anatomic landmarks in normal posterior segment spectral-domain optical coherence tomography: the IN• OCT consensus. *Ophthalmology*. 2014;121(8):1572–1578.

37. Karampelas M, Sim DA, Keane PA, et al. Evaluation of retinal pigment epithelium–Bruch's membrane complex thickness in dry age-related macular degeneration using optical coherence tomography. *Br J Ophthalmol*. 2013;97(10):1256–1261.

38. Brandl C, Brücklmayer C, Günther F, et al. Retinal layer thicknesses in early age-related macular degeneration: results from the German AugUR Study. *Invest Ophthalmol Vis Sci*. 2019;60(5):1581–1594.

39. Curcio CA, Messinger JD, Sloan KR, Mitra A, McGwin G, Spaide RF. Human chorioretinal layer thicknesses measured in macula-wide, high-resolution histologic sections. *Invest Ophthalmol Vis Sci*. 2011;52(7):3943–3954.

40. Trinh M, Kalloniatis M, Alonso-Caneiro D, Nivison-Smith L. High-density optical coherence tomography analysis provides insights into early/intermediate age-related macular degeneration retinal layer changes. *Invest Ophthalmol Vis Sci*. 2022;63(5):36.

41. Aytulun A, Cruz-Herranz A, Aktas O, et al. APOSTEL 2.0 recommendations for reporting quantitative optical coherence tomography studies. *Neurology*. 2021;97(2):68–79.

42. Waldstein SM, Vogl W-D, Bogunovic H, Sadeghipour A, Riedl S, Schmidt-Erfurth U. Characterization of drusen and hyperreflective foci as biomarkers for disease progression in age-related macular degeneration using artificial intelligence in optical coherence tomography. *JAMA Ophthalmol*. 2020;138(7):740–747.

43. Anderson DH, Mullins RF, Hageman GS, Johnson LV. A role for local inflammation in the formation of drusen in the aging eye. *Am J Ophthalmol*. 2002;134(3):411–431.

44. Crabb JW, Miyagi M, Gu X, et al. Drusen proteome analysis: an approach to the etiology of age-related macular degeneration. *Proc Nat Acad Sci*. 2002;99(23):14682–14687.

45. Kijlstra A, La Heij E, Hendrikse F. Review article, immunological factors in the pathogenesis and treatment of age-related macular degeneration. *Ocul Immunol Inflamm*. 2005;13(1):3–11.

46. Telander DG. *Inflammation and age-related macular degeneration (AMD)*. Milton Park, Oxfordshire: Taylor & Francis; 2011:192–197.

47. Gheorghe A, Mahdi L, Musat O. Age-related macular degeneration. *Romanian J Ophthalmol*. 2015;59(2):74.

48. Chen H, Anderson RE. Metabolism in frog retinal pigment epithelium of docosahexaenoic and arachidonic acids derived from rod outer segment membranes. *Exp Eye Res*. 1993;57(3):369–377.

49. Gordon WC, de Turco EBR, Bazan NG. Retinal pigment epithelial cells play a central role in the conservation of docosahexaenoic acid by photoreceptor cells after shedding and phagocytosis. *Curr Eye Res*. 1992;11(1):73–83.

50. Chen L, Messinger JD, Kar D, Duncan JL, Curcio CA. Biometrics, impact, and significance of basal linear deposit and subretinal drusenoid deposit in age-related macular degeneration. *Invest Ophthalmol Vis Sci*. 2021;62(1):33.

51. Zarubina AV, Neely DC, Clark ME, et al. Prevalence of subretinal drusenoid deposits in older persons with and

without age-related macular degeneration, by multimodal imaging. *Ophthalmology*. 2016;123(5):1090–1100.

52. Chan H, Cougnard-Grégoire A, Delyfer MN, et al. Multimodal imaging of reticular pseudodrusen in a population-based setting: the Alienor Study. *Invest Ophthalmol Vis Sci*. 2016;57(7):3058–3065.

53. Buitendijk GH, Hooghart AJ, Brussee C, et al. Epidemiology of reticular pseudodrusen in age-related macular degeneration: the Rotterdam Study. *Invest Ophthalmol Vis Sci*. 2016;57(13):5593–5601.

54. Nittala MG, Song YE, Sardell R, et al. Baseline spectral domain optical coherence tomography characteristics of age-related macular degeneration. *Retina (Philadelphia, Pa)*. 2019;39(8):1540.

55. Wood A, Binns A, Margrain T, et al. Retinal and choroidal thickness in early age-related macular degeneration. *Am J Ophthalmol*. 2011;152(6):1030–1038.e2.

56. Lee JY, Lee DH, Lee JY, Yoon YH. Correlation between subfoveal choroidal thickness and the severity or progression of nonexudative age-related macular degeneration. *Invest Ophthalmol Vis Sci*. 2013;54(12):7812–7818.

57. Sasaki M, Ito Y, Yamasaki T, et al. Association of choroidal thickness with intermediate age-related macular degeneration in a Japanese population. *Ophthalmol Retina*. 2021;5(6):528–535.

58. Sigler EJ, Randolph JC. Comparison of macular choroidal thickness among patients older than age 65 with early atrophic age-related macular degeneration and normals. *Invest Ophthalmol Vis Sci*. 2013;54(9):6307–6313.

59. Switzer DW, Jr, MendonÇa LS, Saito M, Zweifel SA, Spaide RF. Segregation of ophthalmoscopic characteristics according to choroidal thickness in patients with early age-related macular degeneration. *Retina*. 2012;32(7):1265–1271.

60. Chung SE, Kang SW, Lee JH, Kim YT. Choroidal thickness in polypoidal choroidal vasculopathy and exudative age-related macular degeneration. *Ophthalmology*. 2011;118(5):840–845.

61. Kim S-W, Oh J, Kwon S-S, Yoo J, Huh K. Comparison of choroidal thickness among patients with healthy eyes, early age-related maculopathy, neovascular age-related macular degeneration, central serous chorioretinopathy, and polypoidal choroidal vasculopathy. *Retina*. 2011;31(9):1904–1911.

62. Manjunath V, Goren J, Fujimoto JG, Duker JS. Analysis of choroidal thickness in age-related macular degeneration using spectral-domain optical coherence tomography. *Am J Ophthalmol*. 2011;152(4):663–668.

63. Arnold JJ, Sarks SH, Killingsworth MC, Sarks JP. Reticular pseudodrusen: a risk factor in age-related maculopathy. *Retina*. 1995;15(3):183–191.

64. Margolis R, Spaide RF. A pilot study of enhanced depth imaging optical coherence tomography of the choroid in normal eyes. *Am J Ophthalmol*. 2009;147(5):811–815.

65. Sarks S. Changes in the region of the choriocapillaris in ageing and degeneration. *XXIII Concilium Ophthalmologicum, Kyoto*. 1978:228–238.

66. Ramrattan RS, van der Schaft TL, Mooy CM, De Bruijn W, Mulder P, De Jong P. Morphometric analysis of Bruch's membrane, the choriocapillaris, and the choroid in aging. *Invest Ophthalmol Vis Sci*. 1994;35(6):2857–2864.

67. Mullins RF, Johnson MN, Faidley EA, Skeie JM, Huang J. Choriocapillaris vascular dropout related to density of drusen in human eyes with early age-related macular degeneration. *Invest Ophthalmol Vis Sci*. 2011;52(3):1606–1612.

68. Seddon JM, McLeod DS, Bhutto IA, et al. Histopathological insights into choroidal vascular loss in clinically documented cases of age-related macular degeneration. *JAMA Ophthalmol*. 2016;134(11):1272–1280.

69. Nassisi M, Tepelus T, Nittala MG, Sadda SR. Choriocapillaris flow impairment predicts the development and enlargement of drusen. *Graefes Arch Clin Exp Ophthalmol*. 2019;257:2079–2085.

70. Nassisi M, Tepelus T, Corradetti G, Sadda SR. Relationship between choriocapillaris flow and scotopic microperimetry in early and intermediate age-related macular degeneration. *Am J Ophthalmol*. 2021;222:302–309.

71. Corradetti G, Tiosano L, Nassisi M, et al. Scotopic microperimetric sensitivity and inner choroid flow deficits as predictors of progression to nascent geographic atrophy. *Br J Ophthalmol*. 2021;105(11):1584–1590.

72. Mahmoudi A, Corradetti G, Emamverdi M, et al. Atrophic lesions associated with age-related macular degeneration: high-resolution versus standard OCT. *Ophthalmol Retina*. 2023;8:367–375.